Available online at www.sciencedirect.com

SCIENCE DIRECT®

Polymer 46 (2005) 229–236

polymer

www.elsevier.com/locate/polymer

Radiochemical ageing of an amine cured epoxy network. Part I: change of physical properties

T. Devanne[a], A. Bry[a], L. Audouin[b,*], J. Verdu[b]

[a]Commissariat à l'Energie Atomique, BP 16, 37260 Monts, France
[b]Laboratoire de Transformation et Vieillissement des Polymères, ENSAM, 151 Boulevard de l'Hôpital, 75013 Paris, France

Received 2 December 2003; received in revised form 9 July 2004; accepted 9 July 2004

Abstract

An aromatic rich, amine cured epoxy network (initial glass transition temperature 250 °C), was irradiated in air (pressure 0.22 MPa), at 30 and 120 °C, by gamma rays with two dose rates 2 and 20 kGy/h, for doses upto 70 MGy. The following characteristics were recorded, thickness of oxidised layer (TOL) from IR microspectrophotometry, flexural strength σ_R, toughness K_{IC} and glass transition temperature T_g. σ_R decreases from 120 MPa to about 40 MPa in the most degraded samples. This decrease is sharply linked to TOL showing the key role of the oxidised layer in crack initiation. K_{IC} decreases from 0.7 to 0.55 MPa m$^{1/2}$. Data are too much scattered to allow a kinetic study but it appears that, in the early period of exposure, K_{IC} decreases more rapidly at 120 °C than at 30 °C. T_g decreases from 250 to 140 °C in the most degraded samples, and the decrease is faster at 30 °C than at 120 °C. The decrease of T_g is attributed to a predominant chain scission process. The decrease of K_{IC} can be attributed to a combination of chain scission and physical ageing or chain scission and crosslinking. A relationship between T_g and the number of chain scissions, derived from the Di Marzio's theory, is proposed.

Keywords: Epoxy network; Crosslink density; Radiochemical degradation

1. Introduction

After four decades (1950–1990) of intense scientific production, the domain of polymer radiochemical ageing was characterised, in last 15 years, by decreasing and almost sporadic activity. The main elementary processes are now relatively well understood but problems of lifetime prediction remain largely open, essentially because they are at the boundary of many scientific fields: ageing mechanisms (eventually radical chemistry), kinetics (chain processes with diffusion-reaction coupling) and materials science (consequences of structural modifications on use properties). Synthetic approaches of these problems, aimed to reduce empirisme in lifetime prediction, are now favoured by a certain revival (at least in France) induced by the growing interest for sustainable development.

Among industrial polymers, thermosets and especially epoxies, given rise to a very scarce literature focused on both extremities of research field, i.e. organic chemistry on one side and mechanical properties (composites) on the other side with practically no interconnection between both domains. The present article deals with the study of a new epoxy network with an especially high aromatic content, and it will be tried to have a specific approach trying to take into account all the important aspects of lifetime prediction.

This main available research results on epoxy radiochemical ageing can be summarised as follows:

(a) Ageing results essentially from radical process. Relatively long lived radicals can be observed by ESR [1] in irradiated epoxy networks.

(b) As predicted from well-known structure–stability relationships, the weakest part of these networks is the aliphatic part, i.e. in all cases, the isopropanol segment: –CH_2–CH(OH)–CH_2–, and when aliphatic amines are used, the corresponding hydrocarbon segments, for instance dimethylene sequences in the case of ethylene diamine

---

* Corresponding author. Tel.: +33-1-44-24-64-13; fax: +33-1-44-24-63-82.

E-mail address: ltvp@paris.ensam.fr (L. Audouin).

0032-3861/$ - see front matter © 2004 Elsevier Ltd. All rights reserved.
doi:10.1016/j.polymer.2004.07.039

(EDA) [2] or triethylenetetramine (TETA) [3]. Irradiation in inert atmosphere leads to H_2 evolution, linked presumably to the fact that homolysis of CH bonds is an important primary event:

$$PH + h\nu \rightarrow P^{\bullet} + H^{\bullet} \quad (1)$$

$$H^{\bullet} + PH \rightarrow P^{\bullet} + H_2 \quad (2)$$

In the presence of oxygen, these processes initiate radical chains leading to oxygen containing groups such as hydroperoxides, ketones, acids, etc. which are easily observable by IR spectrophotometry [2,3].

(c) Despite their higher stability, aromatic groups are also attacked, for instance the bisphenol A moiety in diglycidyl ether of bisphenol A (DGEBA) systems [2,4]. Discoloration [5,6] results presumably from the formation of conjugated species resulting from the attack of aromatic groups but the overall stability, as judged by the rate of carbonyl build-up or the loss of mechanical properties, is an increasing function of the aromatic content. The lifetime increases by a factor three [3] or ten [7] when aliphatic hardener TETA [3] or DETA [7] is replaced by diaminodiphenyl methane (DDM). The aromatic groups can be promoted to excited states which are able to transfer their energy to the rest of the network [8].

(d) Most of the time, radiochemical ageing tries are performed directly on composites of industrial interest and ageing effects are judged from mechanical tests [9–17] which gives information directly usable in practice, but generally difficult to interpret in terms of mechanisms. As a matter of fact, the following difficulties are generally found: (i) analytical difficulties due to the presence of fibres and to the matrix insolubility; (ii) lack of theoretical knowledge on structure–property relationships for thermosets [18]; (iii) possible effects of radiochemically induced changes in the matrix-fibre interphase on the mechanical behaviour [16, 17], and (iv) the wide variety of compositions and structural states (degree of cure, presence of structural irregularities due to side reactions during cure, thermodynamical state of the matrix linked to its thermomechanical story) increase again the complexity of the problem making difficult, or even impossible, the synthesis of the results.

(e) It is, however, generally recognised that the mechanical behaviour of thermosets depends more or less sharply of their crosslink density. Here, spectrochemical methods lack generally to give useful information but, glass transition temperature (T_g or T_α from dynamic mechanical analysis) changes are relatively easy to determine and can be interpreted in terms of modifications of the network structure (chain scission or crosslinking). Experimental data [19–21] seem to show that T_g decreases generally in amine cured epoxies, indicating a predominant chain scission process.

In most of the above cited articles, however, there is no kinetic analysis of the ageing process. When lifetimes are reported, they are generally expressed in terms of lethal dose at temperature close to the ambient temperature. Furthermore, endlife criteria such as loss of 50% of the ultimate elongation, as reported by Wilski [22], are questionable. Is the lethal dose independent of the dose rate? And temperature? What is the shape of the curve mechanical property versus dose? Are the reported endlife criteria pertinent? It appears impossible to answer these questions without a kinetic model. This latter could be based on the following sequence (Fig. 1):

The aim of our study is to try to build a kinetic model for the radiochemical degradation of a highly aromatic epoxide–amine network designed to combine a high T_g with a good thermal and radiochemical stability. In the first part, the changes of T_g and mechanical properties will be presented and attention will be paid to the eventual effects of a superficial oxidation. In the second part, a kinetic model will be proposed and its main parameters will be determined, essentially from NMR and ESR experiments.

2. Experimental

2.1. Materials

The network under study is based on the stoichiometric combination of a 50/50 (molar) mixture of two epoxide monomers—Tactix 742 (from Ciba) and resorcinol diglycidyl ether (RDE) (from Sigma Aldrich)—with diamino diphenyl sulphone (DDS) (from Ciba). Chemical structures of these products are given in Fig. 2. Their chemical and chromatographic analysis showed that their degree of purity was higher than 95% so that they were used without purification. The monomer mixture was first molten and stirred at 90 °C. It was then cast on aluminium moulds to obtain plates of $40\times20\times2\ \text{cm}^3$, which were cured 30 min at 150 °C, 1 h at 180 °C and 2 h at 260 °C under nitrogen. In these conditions, no residual cure exotherm can be observed by DSC indicating a quasi complete polycondensation. Cured plates were machined under water to give parallelepipedic samples of $60\times10\times3\ \text{mm}^3$. The samples of red colour are transparent and free of bubbles and other visible defects.

2.2. Irradiations

Irradiations were performed in dry air using gamma rays from Co^{60} sources. The air pressure in the reactor was 0.22 MPa. Four irradiation tests combining two dose rates and two temperatures were performed. The exposure conditions are reported in Table 1. Dose rates were determined using cellulose triacetate films, just before irradiation. The measurement incertitude is $\pm15\%$. Between irradiation and characterisation, samples were stored under inert atmosphere at -26 °C to minimise post-irradiation effects.

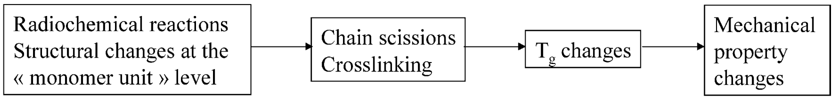

Fig. 1. Schematisation of the approach used for kinetic modelling.

Table 1
Irradiation conditions

Dose rate (kGy/h)	Temperature (°C)	Dose (MGy)
2	30	0–10
20	30	0–70
2	120	0–10
20	120	0–70

2.3. Measurements

For mechanical characterisations, the three points bending test according to French Standard AFNOR NFT 5100 was chosen. An Instron 4500 machine was used at a crosshead speed of 1.5 mm/min with a span length of 50 mm. Results reported here are the average of three measurements made on three different samples. The fracture toughness was determined according to ISO Standard 13586, in the SENB geometry. The cross-head speed was set at 10 mm/min, span length at 40 mm. Three to seven samples per measure were tested. The initial crack length was determined optically after the try. Viscoelastic properties were determined using a Rheometrics RDA III apparatus in torsional mode at 1 Hz frequency, with a temperature ramp of 5 °C/min between 423 and 573 K. The glass transition temperature T_g (in fact T_α) is taken at the inflection point of the storage modulus–temperature curve. The thickness of the oxidised layer was determined by FT-IR microspectrophotometry. A sample section is polished using sandpaper until a thickness of 10–15 μm (measured with an electronic micrometer Cadar MS25RS). Then, it is analysed on an Equinox 55 Bruker spectrophotometer in ATR mode, using a Golden Gate Diamond cell from Grasby Specac Co. A spectrum (32 scans at $2\ \mathrm{cm}^{-1}$) is taken for each step. The extent of oxidation was appreciated from the absorbance of carbonyl groups at $1725\ \mathrm{cm}^{-1}$ using the aromatic peak at $1600\ \mathrm{cm}^{-1}$ as internal standard. The reduced absorbance A_{CO} decreases pseudo exponentially

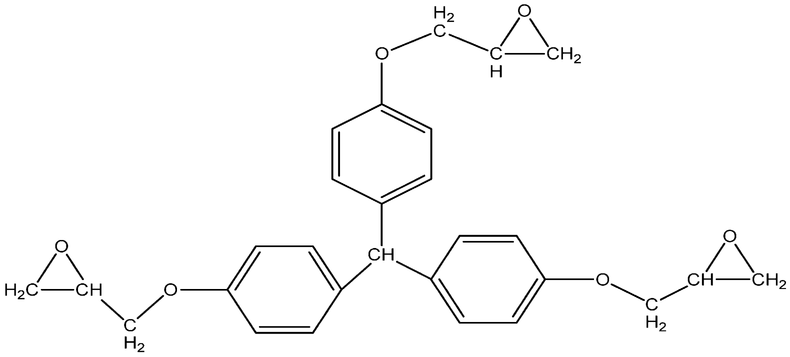

Tactix 742

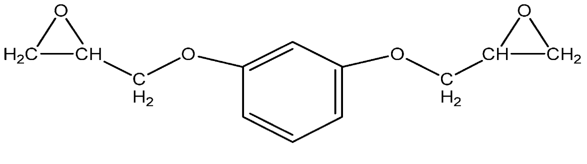

Resorcinol Diglycidyl Ether

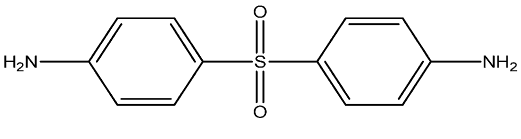

Diamino Diphenyl Sulphone

Fig. 2. Chemical structure of monomers.

from the surface to the core. The thickness of the oxidised layer was arbitrarily assimilated to the depth of the layer where $A_{CO}=A_{Cos}/2.718$, A_{Cos} being the reduced absorbance at the surface.

3. Results and discussion

3.1. Thickness of the oxidised layer

The thickness of the oxidised layer (TOL) has been plotted versus radiation dose in Fig. 3, which calls for the following comments:

(i) Curves display a horizontal plateau characterising the existence of a stationary state for the diffusion-reaction process. The height of this plateau increases with the temperature and decreases with the dose rate. In the stationary state, the TOL values are 25 ± 5 μm at 20 kGy/h, 30 °C; 45 ± 5 μm at 20 kGy/h, 120 °C and 55 ± 5 μm at 2 kGy/h, 120 °C. For 2 kGy/h, 30 °C, the plateau was not reached but the curve tends to be above the curve obtained at 20 kGy/h, 30 °C.

(ii) The initial part of the curve corresponds to a transient which can be modelled suppressing the stationary state hypothesis in kinetic equations [23] (which needs a numerical resolution). It will not be studied here. The main trends of variation of the TOL with the exposure conditions can be discussed on the basis of a simplified theory of diffusion controlled oxidation [24] according which it can be written:

$$\mathrm{TOL} = \sqrt{\frac{DC(\mathrm{O}_2)}{R(\mathrm{O}_2)}} \tag{1}$$

where D is the oxygen diffusion coefficient into the polymer, $C(\mathrm{O}_2)$ is the equilibrium oxygen concentration in the material and $R(\mathrm{O}_2)$ is the consumption rate of oxygen. According to Henry's law:

$$C(\mathrm{O}_2) = P(\mathrm{O}_2)S \tag{2}$$

where S is the solubility coefficient of O_2 in the polymer and $P(\mathrm{O}_2)$ is the oxygen partial pressure in the atmosphere (0.044 MPa in our case). According to simplest kinetic models, assuming oxygen excess, bimolecular termination, hydroperoxide stability and long kinetic chain, the whole oxidation rate is expected to be proportional to the square root of the initiation rate, this latter being proportional to the dose rate, so that:

$$R(\mathrm{O}_2) = K\sqrt{I} \tag{3}$$

where I is the dose rate and K a constant.

Using Eqs. (1–3), it can be written:

$$\mathrm{TOL} = A\frac{P^{1/2}}{I^{1/4}} \tag{4}$$

where $A=(DS/K)^{1/2}$. Thus at a given temperature, it is possible to build a mastercurve corresponding to reference conditions, for instance $I_R=2$ kGy/h and $P_R=2\times10^4$ Pa, using:

$$\frac{\mathrm{TOL_R}}{\mathrm{TOL}} = \left(\frac{I}{I_R}\right)^{1/4} \times \left(\frac{P_R}{P}\right)^{1/2} \tag{5}$$

The mastercurves at 120 and 30 °C are presented in Fig. 4.

They could be reduced to a single mastercurve, using a shift factor obeying to Arrhenius law, with an apparent activation energy H of about 7.5 kJ/mol. The equation of this mastercurve at the reference temperature T_R would be:

$$(\mathrm{TOL})_u = \left[\left(\frac{I}{I_R}\right)^{1/4}\left(\frac{P_R}{P}\right)^{1/2}\exp\left(-\frac{H}{R}\left(\frac{1}{T_R}-\frac{1}{T}\right)\right)\right]\mathrm{TOL} \tag{6}$$

3.2. Fracture properties

The flexural stress at break σ_R was plotted versus dose in Fig. 5.

Here, dose rate effects are difficult to appreciate, but temperature effects are spectacular: at 120 °C, the stress at break decreases rapidly from 120 MPa to about 40 MPa after 10 MGy exposure. Then it remains almost constant

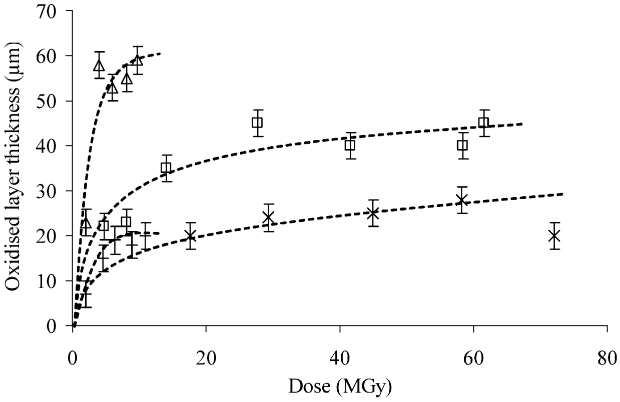

Fig. 3. Dose dependance of the oxidised layer thickness (+ 2 kGy/h, 30 °C; × 20 kGy/h, 30 °C; △ 2 kGy/h, 120 °C; □ 20 kGy/h, 120 °C).

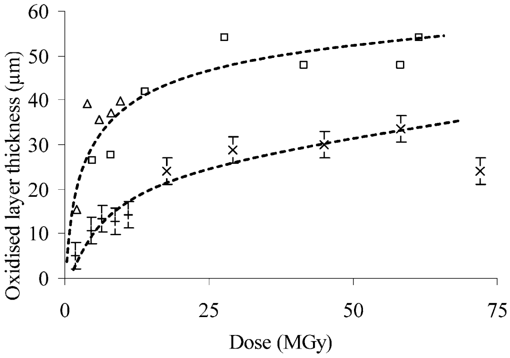

Fig. 4. Mastercurves of oxidised layer thickness (+ 2 kGy/h, 30 °C; × 20 kGy/h, 30 °C; △ 2 kGy/h, 120 °C; □ 20 kGy/h, 120 °C).

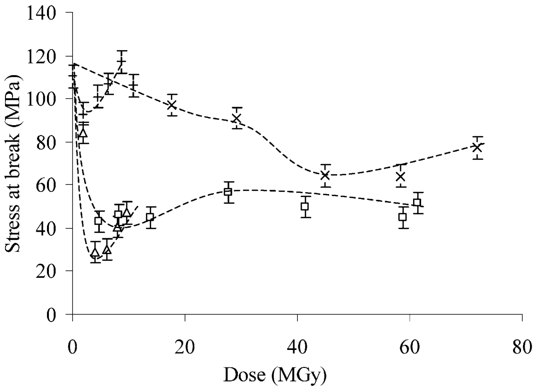

Fig. 5. Dose dependence of flexural stress at break (+ 2 kGy/h, 30 °C; × 20 kGy/h, 30 °C; △ 2 kGy/h, 120 °C; □ 20 kGy/h, 120 °C).

until 70 MGy. At 30 °C, a pseudo induction period of about 10 MGy can be observed, then σ_R decreases slowly to reach 60–70 MPa after 70 MGy exposure. Two characteristics can be involved in such an embrittlement process: (i) a decrease of the material's toughness linked to radiation induced structural changes homogeneously distributed into the sample volume, and/or (ii) the build-up of defects having a sufficient size to initiate fracture. Both characteristics are linked by the basic laws of fracture mechanics:

$$\sigma_R = \left(\frac{2Ee}{\pi a}\right)^{1/2} = \frac{K_{IC}}{Y(\pi a)^{1/2}} \tag{7}$$

where E is the tensile modulus, e the surface energy, a the defect size and Y a geometric factor depending of the notch size and the sample width.

Toughness measurements leaded to the results of Fig. 6 in which K_{IC} decreases from 0.7 MPa m$^{1/2}$ to about 0.55 MPa m$^{1/2}$ after 70 MGy exposure, whatever the exposure conditions.

It is clear that at 120 °C, the relative variation of σ_R ($\sim$60%) is considerably higher than the relative variation of K_{IC} ($\sim$20%), showing that ageing at 120 °C creates large size defects or increases the size of pre-existing defects. σ_R was plotted versus TOL in Fig. 7.

One observes in Fig. 7 the existence of two distinct states: the initial state ($\sigma_R \sim 120$ MPa) corresponding to unchanged fracture properties and the 'brittle' state ($\sigma_R \sim 40$ MPa) corresponding to highly degraded samples (at 120 °C) for which σ_R is almost independent of TOL or decreases slowly with TOL. Between both states, one can observe a transition zone corresponding roughly to 10 μm < TOL < 30 μm. The whole results of mechanical tests can be tentatively interpreted as follows: ageing of the non-oxygenated sample core leads to a limited decrease of the toughness (typically less than 25% in the case under study). For irradiation made at 30 °C, the thickness of the oxidised layer remains generally lower than 30 μm, a value close to the critical defect size for embrittlement. Thus, the oxidised layer plays a small role in crack initiation; the decrease of fracture properties is essentially dominated by the consequences of radiochemical degradation in the bulk. In contrast, for irradiation at 120 °C, the thickness of the oxidised layer is significantly higher than the critical defect size, so that the oxidised layer plays fully its crack initiation role, which leads to a fast decrease of the flexural strength at break in the early period of exposure. How to apply these results in practice? Let us consider the main applications of epoxy resins: adhesives and composites. In the case of adhesives, only small portions of the surface are exposed to air, most of the ageing processes are anaerobic. In the case of composites, K_{IC} is very high, typically 10–100 times the values obtained here, owing to the reinforcing effect of fibres. Then, oxidised superficial layers of few dozens of micrometers cannot affect the whole fracture behaviour. Thus, in most of practical cases, the most important effect is the less spectacular one, i.e. the effect of anaerobic ageing in the bulk on fracture properties. A way to study this process consists of recording the glass transition temperature variations.

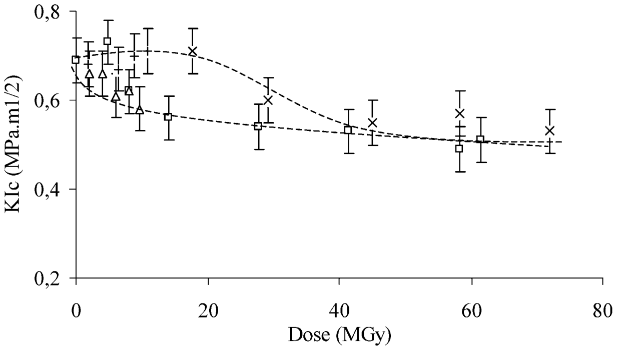

Fig. 6. Dose dependence of fracture toughness (+ 2 kGy/h, 30 °C; × 20 kGy/h, 30 °C; △ 2 kGy/h, 120 °C; □ 20 kGy/h, 120 °C).

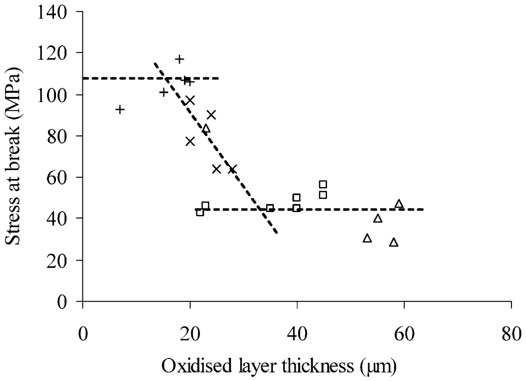

Fig. 7. Variation of the stress at break versus the oxidised layer thickness (+ 2 kGy/h, 30 °C; × 20 kGy/h, 30 °C; △ 2 kGy/h, 120 °C; □ 20 kGy/h, 120 °C).

3.3. Glass transition temperature

The glass transition temperature T_g was determined by DMA in conditions where essentially the bulk sample properties were recorded. T_g is plotted versus dose in Fig. 8.

T_g decreases in all cases, indicating that the polymer

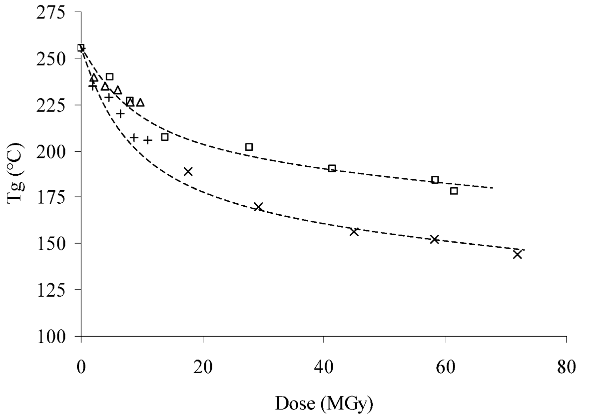

Fig. 8. Dose dependence of the glass transition temperature (+ 2 kGy/h, 30 °C; × 20 kGy/h, 30 °C; △ 2 kGy/h, 120 °C; □ 20 kGy/h, 120 °C).

undergoes predominant chain scission. At each temperature of exposure, all the points are close to a single curve, suggesting that the phenomenon responsible for T_g decrease is dose rate independent (that is not surprising for a radiolytic process). The phenomenon seems to be auto-retardated but this is, at least partially, determined by the structure–T_g relationship (see below). The most surprising fact is, no doubt, the effect of temperature: T_g decreases more rapidly at 30 °C than at 120 °C. Using simplifying hypotheses, it is possible to envisage a translation of T_g data in terms of crosslink density data using Di Marzio's equation [25]. It has been proved that this equation has an excellent predictive value in the case of epoxy networks [26]. This equation can be written:

$$n = \frac{1}{KF}\left(1 - \frac{T_{gl}}{T_g}\right) \tag{8}$$

where K is an universal constant ($K = 2.91$), F is the molar mass per rotatable bond (called Flex Parameter by Di Marzio), T_{gl} the T_g of a hypothetical linear copolymer containing all the structural units of the network except crosslinks. Using the method of Bellenger et al. [26], it was found $F = 30$ g/mol, $T_{gl} = 348$ K for the initial (non-degraded) network. Eq. (8) can be used to determine the crosslink density changes during ageing if the following hypotheses are valid:

(i) Di Marzio's equation can be applied to degraded networks (i.e. networks containing dangling chains) provided that the copolymer effect of dangling chains is the same as for elastically active chains: a chain scission modifies the crosslink density but not T_{gl} and F. This hypothesis is valid at low conversions but probably not at high conversions. Studies of non-stoichiometric networks seem to reveal some physical crosslinking effect of dangling chains [27]. In other words, crosslink density values could be overestimated at high conversions.

(ii) Eventual reactions modifying lateral groups without chain scission do not modify significantly F and T_{gl}. This hypothesis can be checked by spectrochemical investigations: IR or NMR (see the second part of this paper). Effectively, the molecular structure of the network is essentially preserved, so that no significant changes of chain stiffness, susceptible to influence F or T_{gl}, are expected.

(iii) It is supposed, in a first approach, that the network under study undergoes a 'pure' chain scission process (no simultaneous crosslinking).

In such networks with trifunctional crosslinks, one chain scission s leads to the disappearance of two crosslinks n:

$$\frac{dn}{dt} = -2\frac{ds}{dt} \tag{9}$$

Therefore:

$$\frac{dT_g}{dn} = \frac{dT_g}{dt} / \frac{dn}{dt} = -\frac{1}{2}\frac{dT_g}{dt} / \frac{ds}{dt} \tag{10}$$

By derivation of Eq. (8), one obtains:

$$\frac{dT_g}{dn} = KF\frac{T_g^2}{T_{gl}} \tag{11}$$

So that:

$$\frac{ds}{dt} = \frac{T_{gl}}{2KF}\frac{1}{T_g^2}\frac{dT_g}{dt} \tag{12}$$

By integrating, one obtains:

$$s = \frac{T_{gl}}{2KF}\left(\frac{1}{T_g} - \frac{1}{T_{g0}}\right) \tag{13}$$

where T_{g0} is the initial value of T_g. The calculated values of s are plotted versus dose in Fig. 9.

Curves display a negative concavity showing that the rate of chain scission is a decreasing function of the conversion. This characteristic can be partially linked to the facts that (i) the correction due to dangling chains has not been made on Di Marzio's equation, (ii) the higher the conversion, the higher the probability to have a chain scission on a dangling chain, i.e. the lower the probability to have a chain scission on an elastically active chain leading to a crosslink density decrease. These complications are not insuperable so that a way to predict the consequences of irradiation on physical properties such as T_g is open. The corresponding kinetic model will be presented in the second part of this paper. But,

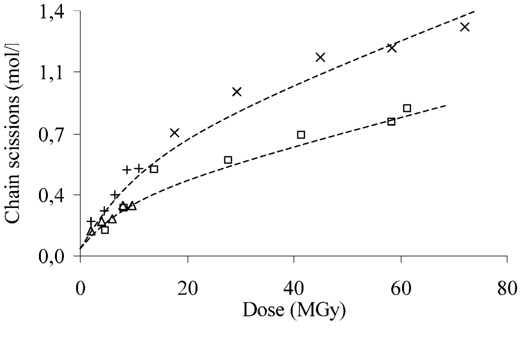

Fig. 9. Dose dependence of the number of chain scissions (+ 2 kGy/h, 30 °C; × 20 kGy/h, 30 °C; △ 2 kGy/h, 120 °C; □ 20 kGy/h, 120 °C).

is it possible to go beyond T_g and to predict for instance K_{IC} from the number of chain scissions? Literature reviews on this topic show that the structure–toughness relationships are not well established for networks [28]. In the case of ideal networks, it is clear that K_{IC} tends to increase when T_g decreases [29]. But, in non-ideal networks such as non-stoichiometric epoxide–amine networks, K_{IC} decreases rapidly with the concentration of dangling chains [30] (epoxide excess). In the case under study, where chain scission creates dangling chains, K_{IC} would be expected to decrease (as effectively observed) in the same way as T_g. This is not the case since a change of the temperature of exposure has adverse effects on T_g and K_{IC}. It seems that chain scission is not the unique process influencing K_{IC}. Two hypotheses come in mind:

(i) Physical ageing affects K_{IC} at 120 °C whereas it is negligible at 30 °C. Thus, the change of K_{IC} would result only of chain scission at 30 °C and of combined effects of chain scission and physical ageing at 120 °C. It is well known that physical ageing, which reduces molecular mobility, can lead to a marked toughness decrease in epoxy networks [31].

(ii) Crosslinking occurs simultaneously with chain scission and leads to the broadening of the M_e (molar mass of elastically active chains EAC) distribution. The formation of EAC shorter than initial ones, i.e. with lower maximum elongation, could explain the observed toughness decrease (Fig. 10).

Complementary investigations are needed to elucidate the lack of correlation between glass transition temperature and toughness changes.

4. Conclusion

The aromatic rich epoxy network under study has been exposed to gamma rays at dose rates of 2 and 20 kGy/h and temperatures of 30 and 120 °C, the air pressure being 0.22 MPa. Physical properties such as the glass transition temperature T_g, the flexural strength at break σ_R and the toughness (critical stress intensity factor in mode I: K_{IC}) have been recorded over doses up to 70 MGy. The thickness of the oxidised layer (TOL) has been determined by IR spectrophotometry. TOL is higher at 120 °C than at 30 °C and decreases with dose rates according to a power law $TOL \propto I^{1/4}$. The flexural strength appears to be sharply linked to TOL, showing that the superficial layer is deeply embrittled by oxidation and works as an equivalent notch. The critical size of this latter would be of the order of 25 μm. The toughness is independent of TOL since it is measured on prenotched samples. It decreases from 0.7 to 0.55 MPa m$^{1/2}$. The results are too scattered to permit a kinetic study, but it is clear that, in the early period of exposure, K_{IC} decreases more rapidly at 120 °C than at 30 °C. The glass transition temperature of the non-oxidised sample core decreases as a result of chain scission. The number of chain scissions has been evaluated from T_g decrease, using Di Marzio's law. The rate of chain scission is lower at 120 °C than at 30 °C and decreases with exposure time, but this latter effect could be due to some effect of dangling chains not taken into account in Di Marzio's law. The lack of correlation between T_g and K_{IC} changes could be due to an effect of physical ageing on K_{IC} at 120 °C or to the occurrence of a crosslinking process.

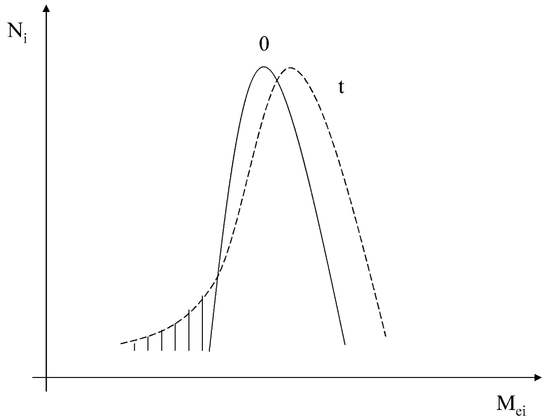

Fig. 10. Schematisation of the distribution of molar masses of elastically active chains before (0) and after (b) ageing in the case of combined crosslinking and chain scission (this latter being predominant). The formation of short chains (broken part) could explain the toughness decrease.

References

[1] Seo KS, Fornes RE, Gilbert RD, Memory JD. J Polym Sci: Part B Polym Phys 1988;26:533.
[2] Burnay SG. Radiat Phys Chem 1980;16(5):389.
[3] Y. Ngono, Comportement à long terme de résine thermodurcissable en milieu irradiant: rôle et action de l'eau, PhD Thesis, University Joseph Fourier; Sept. 1999, Grenoble (France).
[4] Hegazy ESA, Sasuga T, Nishi M, Seguchi T. Polymer 1992;33:2897.
[5] Fouracre RA, Banrord HM, Tedford DJ, Gedeon S, Cao X, Wu S, Fu L. Radiat Phys Chem 1991;37(4):581.
[6] Allattabi A, Fouracre RA, Banrord HM, Tedford DJ. Radiat Phys Chem 1992;40(5):411.
[7] Burnay SG. Radiat Phys Chem 1982;19(2):93.
[8] Tagawa S, Washio M, Hayashi N, Tabata Y. J Nuclear Mater 1985; 133–134:785.
[9] Evans D, Murgaw JT. Adv Cryogenic Engng 1984;30:89.
[10] Dole M. Radiat Phys Chem 1991;37(1):65.
[11] Gilfrish HP, Wilski H. Radiat Phys Chem Int J Radiat Appl Instrum Part C 1992;39(5):401.
[12] Guarino FS, Hauviller C, Kenny JM. J Macromol Sci Phys B 1999;38: 623.
[13] Fornes RE, Memory JD, Naranong N. J Appl Polym Sci 1981;26: 2061.
[14] Wolf KW, Memory JD, Gilbert RD, Fornes RE. J Appl Phys 1982;54: 5558.
[15] Memory JD, Fornes RE, Gilbert RD. J Reinforced Plastics Compos 1988;7:33.
[16] Nishiura I, Katagiri K, Nishijima S, Okada S, Nakahara S. J Nuclear Mater 1990;174:110.

[17] Park JS, Seo KS, Fornes RE, Gilbert RD. Plast Rubb Process Appl 1988;10:203.

[18] Pascault JP, Sautereau H, Verdu J, Williams RJJ. Thermosetting polymers. New York: Marcel Decker; 2002. Chapter 10–14.

[19] Sasuga T, Udagawa A. Polymer 1991;32(3):402.

[20] Spadaro G, Calderaro E, Rizzo G. Radiat Phys Chem 1984;23(5):613.

[21] L. Vignoud, Evolution des propriétés macroscopiques de deux résines époxydes lors du vieillissement sous irradiation; Nov. 2001, PhD Thesis, University Claude BERNARD, Lyon (France).

[22] Wilski H. In: Clough RL, Shalaby SW, editors. Radiation effects on polymers. ACS Symposium Series, vol. 475. Washington: American Chemical Soceity; 1991.

[23] X. Colin, Modélisation cinétique de la thermooxydation de matériaux polymères et composites à hautes performances thermo-mécaniques; Dec. 2001, PhD Thesis, p. 140, ENSAM, Paris (France).

[24] Audouin L, Langlois V, Verdu J, Debruijn JC. J Mater Sci 1994;29:569.

[25] Di Marzio EA. J Res NBS 1964;68A:611.

[26] Bellenger V, Morel E, Verdu J. J Polym Sci: Polym Phys Ed 1987;B25:1219.

[27] Bellenger V, Dahoui W, Verdu J, Galy J, Won TG, Pascault JP. Polymer 1989;30:2013.

[28] Tcharkhtchi A, Trotignon JP, Verdu J. Macroml Symp 1999;147:221.

[29] Pascault JP, Sautereau H, Verdu J, Williams RJJ. Thermosetting polymers. New York: Marcel Decker; 2002. Chapter 12, p. 350.

[30] Drzal LT. Adv Polym Sci 1986;75(II):4.

[31] Kong ESW. Adv Polym Sci 1986;80:125.